Classification: Biological Sciences/Biochemistry

Fluoroquinolone Interactions with *Mycobacterium tuberculosis* Gyrase: Enhancing Drug Activity Against Wild-Type and Resistant Gyrase

Katie J. Aldred,[b,1] Tim R. Blower,[d,2] Robert J. Kerns,[e] James M. Berger,[d,3] and Neil Osheroff[a,b,c,4]

[a]VA Tennessee Valley Healthcare System, Nashville, TN 37212; Departments of [b]Biochemistry and [c]Medicine (Hematology/Oncology), Vanderbilt University School of Medicine, Nashville, TN 37232-0146; [d]Department of Biophysics and Biophysical Chemistry, Johns Hopkins University School of Medicine, Baltimore, MD 21205-2185; and [e]Division of Medicinal and Natural Products Chemistry University of Iowa College of Pharmacy, Iowa City, IA 52242

The authors declare no conflict of interest.

[1]Present Address: Department of Biology, University of Evansville, Evansville, IN 47722
[2]Present Address: School of Biological and Biomedical Sciences and Department of Chemistry, Durham University, Durham, DH1 3LE, UK
[3]To whom correspondence may be addressed. Email: jmberger@jhmi.edu
[4]To whom correspondence may be addressed. Email: neil.osheroff@vanderbilt.edu

This article contains supporting information online at www.pnas.org

Short Title: Quinolones and *Mycobacterium tuberculosis* Gyrase

ABSTRACT:

Mycobacterium tuberculosis is a significant source of global morbidity and mortality. Moxifloxacin and other fluoroquinolones are important therapeutics for the treatment of tuberculosis, particularly multi-drug resistant infections. In order to guide the development of new quinolone-based agents, it is critical to understand the basis of drug action against *M. tuberculosis* gyrase and how mutations in the enzyme cause resistance. Therefore, we characterized interactions of fluoroquinolones and related drugs with wild-type gyrase and enzymes carrying mutations at $GyrA^{A90}$ and $GyrA^{D94}$. *M. tuberculosis* gyrase lacks a conserved serine that anchors a water-metal ion bridge that is critical for quinolone interactions with other bacterial type II topoisomerases. Despite the fact that the serine is replaced by an alanine ($GyrA^{A90}$) in *M. tuberculosis* gyrase, the bridge still forms and plays a functional role in mediating quinolone-gyrase interactions. Clinically relevant mutations at $GyrA^{A90}$ and $GyrA^{D94}$ cause quinolone resistance by disrupting the bridge-enzyme interaction, thereby decreasing drug affinity. Fluoroquinolone activity against wild-type and resistant enzymes can be enhanced by the introduction of specific groups at the C7 and C8 positions. By dissecting fluoroquinolone-enzyme interactions, we determined that an 8-methyl-moxifloxacin derivative induces high levels of stable cleavage complexes with wild-type gyrase and two common resistant enzymes, $GyrA^{A90V}$ and $GyrA^{D94G}$. 8-Methyl-moxifloxacin was ~2 times more potent than moxifloxacin against wild-type *M. tuberculosis* gyrase and displayed higher activity against the mutant enzymes than moxifloxacin did against wild-type gyrase. This chemical biology approach to defining drug-enzyme interactions has the potential to identify novel drugs with improved activity against tuberculosis.

SIGNIFICANCE STATEMENT:

Moxifloxacin and other fluoroquinolone antibacterials are important anti-tuberculosis therapeutics. Fluoroquinolones kill *Mycobacterium tuberculosis*, the causative agent of tuberculosis, by increasing levels of DNA breaks generated by gyrase, an essential type II topoisomerase that regulates DNA topology. As fluoroquinolone usage in anti-tuberculosis regimens is becoming more pronounced, understanding the basis of drug-gyrase interactions and resistance is becoming more important. Using a mechanism-based chemical biology approach, our work identified critical drug features that mediate fluoroquinolone interactions with *M. tuberculosis* gyrase and determined the biochemical basis for fluoroquinolone resistance caused by the most common clinical mutations in gyrase. These findings allowed us to identify a moxifloxacin derivative that displays enhanced activity against wild-type gyrase and maintains high activity against clinically relevant resistant enzymes.

\body

Tuberculosis is a major cause of morbidity and mortality on a global scale and is second only to HIV/AIDS as the most prolific killer due to a single infectious agent (1). According to the World Health Organization, 9 million people were diagnosed with tuberculosis in 2013, and 1.5 million died from the disease (1). The standard treatment regimen for tuberculosis is a 6-month course that includes a combination of rifampin, isoniazid, pyrazinamide, and ethambutol (2, 3). However, fluoroquinolones are becoming more important in the treatment of tuberculosis and are routinely used in multi-drug resistant cases and in patients who are intolerant of first-line therapy (2, 4, 5). Furthermore, moxifloxacin (a newer generation fluoroquinolone) has shown promising results as a potential first-line agent as part of the PaMZ regimen (PA-824, moxifloxacin, and pyrazinamide), which currently is in clinical trials (6).

Fluoroquinolones are broad-spectrum antibacterials that act by increasing levels of DNA strand breaks generated by type II topoisomerases (7-12). Most bacterial species encode two type II enzymes, gyrase and topoisomerase IV (8, 10, 12-14). In these species, gyrase regulates the superhelical density of the bacterial chromosome and removes torsional stress that is generated ahead of DNA replication forks and transcription complexes, and topoisomerase IV primarily unknots and untangles DNA (11, 15, 16). *Mycobacterium tuberculosis*, the causative agent of tuberculosis, is unusual in that it encodes only gyrase (17). As a result, this enzyme displays functional properties of both type II topoisomerases (18).

Recent structural (19) and functional (20, 21) studies with topoisomerase IV indicate that quinolones interact with bacterial type II enzymes primarily through a water-metal ion bridge. This bridge is formed by a divalent metal ion that is chelated by the C3/C4 keto acid of the drug and stabilized by four water molecules (19). Two of these water molecules are coordinated by a conserved serine and acidic residue (located four positions downstream) in the A subunit of the enzyme. Substitutions in the residues that anchor the bridge are the most prevalent cause of quinolone resistance (10-13, 22-27). In most species, the serine is mutated far more often than the acidic residue.

In contrast to most bacterial species, *M. tuberculosis* gyrase contains an alanine (A90) in place of the conserved serine. This situation raises the issue of whether the water-metal ion bridge can be formed or plays a role in mediating quinolone activity in this species. However, the fact that mutations at A90 and the acidic residue (D94) are associated with clinical quinolone resistance in *M. tuberculosis* (28) suggests that the bridge contributes to quinolone function.

Fluoroquinolones are commonly prescribed for community-acquired pneumonia that is later diagnosed as pulmonary tuberculosis (29). This prior treatment is associated with an increased incidence of fluoroquinolone-resistant disease (30, 31). As the use of fluoroquinolones in treating tuberculosis is becoming more pronounced, understanding the basis of drug-gyrase interactions and resistance is becoming more important. Therefore, we analyzed the interactions of fluoroquinolones and related compounds with wild-type and resistant mutant *M. tuberculosis* gyrase. Results indicate that the water-metal ion bridge is partially functional in wild-type gyrase and that the most common resistance mutations cause a decrease in bridge-mediated drug affinity for the enzyme. In contrast to other species (32, 33), quinolone interactions within the gyrase-cleaved DNA complex depend more heavily on substituents at C7 and C8. Based on an analysis of structure-activity relationships at these two positions, we identified fluoroquinolones that display significantly improved activity against wild-type and resistant *M. tuberculosis* gyrase as compared to moxifloxacin.

Results and Discussion

Gyrase is a heterotetramer comprised of two subunits, GyrA (which contains the active site tyrosine that cleaves and ligates DNA) and GyrB (which contains the ATPase and metal-binding domains) (8, 10, 12-14). To characterize interactions between quinolones and *M. tuberculosis* gyrase, we utilized wild-type enzyme and $GyrA^{A90S}$, $GyrA^{A90V}$, $GyrA^{D94G}$, and $GyrA^{D94H}$. Amino acid residues A90 and D94 occur at the positions that, by sequence homology, are predicted to anchor the water-metal ion bridge if it is used to mediate quinolone-enzyme interactions in this species (19-21). The $GyrA^{A90V}$, $GyrA^{D94G}$, and $GyrA^{D94H}$ proteins contain three of the most common mutations associated with quinolone resistance in clinical isolates of *M. tuberculosis* (28). The $GyrA^{A90S}$ protein replaces the alanine found in the wild-type enzyme with a serine, which is the residue that

serves as a bridge anchor in most bacterial type II topoisomerases. The positions of $GyrA^{A90}$ and $GyrA^{D94}$ relative to bound quinolones are described in the accompanying paper by Blower *et al*. (34).

The GyrB subunit of *M. tuberculosis* gyrase was reannotated based on sequence alignments with 50 other bacterial species (35). It is now believed that the start codon is GTG (rather than ATG), which results in a protein that is 675 amino acids in length, rather than 714 (28). The experiments described in this paper used GyrB that reflects this updated annotation.

Enzymatic Activities of Wild-Type and Quinolone-Resistant Mutant *M. tuberculosis* Gyrase. Before analyzing fluoroquinolone action against the wild-type and $GyrA^{A90S}$, $GyrA^{A90V}$, $GyrA^{D94G}$, and $GyrA^{D94H}$ mutant *M. tuberculosis* gyrase proteins, we determined baseline DNA supercoiling and cleavage activities for the enzymes in the absence of drugs (Figure 1). Each mutant enzyme maintained high DNA supercoiling activity and in the presence of Ca^{2+} (used to increase baseline levels of enzyme-mediated DNA scission) cleaved DNA at least as well as wild-type gyrase. Thus, quinolone resistance does not correlate with a loss of baseline activity for any of the mutant enzymes examined.

Effects of Fluoroquinolones and Related Compounds on DNA Cleavage Mediated by Wild-Type and Fluoroquinolone-Resistant Mutant *M. tuberculosis* Gyrase. The first set of experiments compared the ability of ciprofloxacin and moxifloxacin to induce DNA cleavage by wild-type gyrase and the mutant enzymes (Figure 2, top). The two drugs generated similar levels of cleavage with the wild-type enzyme. In contrast, moxifloxacin maintained higher activity against the $GyrA^{A90V}$, $GyrA^{D94G}$, and $GyrA^{D94H}$ mutant proteins. As shown previously, the D94G and D94H mutations caused a higher level of fluoroquinolone resistance than the A90V mutation (36, 37).

The above findings are consistent with the hypothesis that fluoroquinolones interact with wild-type *M. tuberculosis* gyrase through a water-metal ion bridge that is anchored primarily by D94. To investigate this possibility, the activity of ciprofloxacin and moxifloxacin against $GyrA^{A90S}$ was examined. The inclusion of the serine residue in place of the alanine provides the potential to reconstitute a fully functional bridge. As seen in Figure 2 (top), both fluoroquinolones displayed dramatically higher activity against $GyrA^{A90S}$ than they did against wild-type gyrase: drug potency

(*i.e.*, drug concentration required to induce 50% maximal DNA cleavage) was ~5-fold higher and levels of cleavage at 100 μM were ~2-fold higher. Collectively, these findings suggest that there is sufficient conservation of structure such that *M. tuberculosis* gyrase is capable of using a water-metal ion bridge to mediate fluoroquinolone-enzyme interactions. This conclusion is supported by the structural studies in the accompanying paper by Blower *et al*. (34).

Quinazolinediones are fluoroquinolone-like compounds that lack the C3/C4 keto acid required to chelate metal ions. In several other species, quinazolinediones containing a 3'-(aminomethyl)pyrrolidinyl [3'-(AM)P] (or a related) group at C7 maintain activity against enzymes containing mutations that disrupt the water-metal ion bridge by forming binding interactions primarily through the C7 substituent (20, 21, 32, 38-42). As seen in Figure 2 (middle, left), the activity of 8-methyl-3'-(AM)P-dione is unaffected by mutations that could disrupt or strengthen the water-metal ion bridge in *M. tuberculosis* gyrase. The activity of 8-methyl-3'-(AM)P-FQ (the fluoroquinolone version of this quinazolinedione) is unaffected by bridge-disrupting mutations but is enhanced upon the introduction of the serine residue at position 90 (Figure 2, middle, right). Once again, these findings support the hypothesis that clinically relevant fluoroquinolones interact with *M. tuberculosis* gyrase through the water-metal ion bridge and that D94 likely mediates a partial bridging interaction in the absence of the upstream serine.

Fluoroquinolones that have a C8 substituent generally display better activity against clinical tuberculosis isolates than do derivatives with a C8-H (43, 44). Therefore, 3'-(AM)P-quinazolinedione and -fluoroquinolone derivatives that contained a C8-H were used to examine the influence of the C8 substituent on drug activity (Figure 2, bottom). The activity of 8-H-3'-(AM)P-dione was markedly decreased against all of the enzymes, confirming that the C8 methyl group plays an important role in mediating the activity of these compounds. The activity of 8-H-3'-(AM)P-FQ also decreased with each enzyme as compared to the C8-methyl version of this fluoroquinolone. The relative activity of 8-H-3'-(AM)P-FQ correlated with the capacity of each enzyme to anchor the water-metal ion bridge.

Taken together, the above findings strongly suggest that wild-type *M. tuberculosis* gyrase partially supports the water-metal ion bridge and that the bridge and the C7 and C8 substituents play

important roles in supporting quinolone activity. Therefore, the contributions of these three drug features to quinolone interactions and activity were analyzed in greater detail.

Role of the Water-Metal Ion Bridge in Facilitating Quinolone Activity Against *M. tuberculosis* Gyrase. To determine whether quinolone interactions with *M. tuberculosis* gyrase are mediated by the water-metal ion bridge, Mg^{2+} titrations were carried out to assess the effects of A90 mutations on the metal ion concentration required to support DNA cleavage induced by ciprofloxacin (Figure 3, left). The amino acid at this position plays a critical role in anchoring the water-metal ion bridge in other bacterial type II enzymes (20, 21, 33). Results with wild-type gyrase were compared to those of mutant enzymes containing a serine or a valine in place of the alanine at position 90. The $GyrA^{A90S}$ mutant enzyme, which contains the conserved serine residue found in most other bacterial type II enzymes and greatly enhances fluoroquinolone activity (see Figure 2), required a lower concentration of Mg^{2+} to achieve half-maximal and maximal levels of quinolone-induced DNA cleavage. In marked contrast, the $GyrA^{A90V}$ mutant enzyme, which causes quinolone resistance (see Figure 2), required a higher concentration of Mg^{2+} to achieve half-maximal and maximal levels of quinolone-induced DNA cleavage.

These results demonstrate that the amino acid at position 90 affects the affinity of the divalent metal ion that is chelated by the quinolone and indicate that the water-metal ion bridge is a point of contact between quinolones and *M. tuberculosis* gyrase. It is likely that the alanine at position 90 in wild-type gyrase, while not serving as a bridge anchor, still allows D94 to anchor the bridge. However, because *M. tuberculosis* gyrase has only one available amino acid to anchor the bridge, fluoroquinolone interactions are weaker than seen with species that encode two amino acid bridge anchors (20, 21, 33). Substitution of A90 with the larger valine may cause quinolone resistance by interfering with the ability of water molecules to coordinate properly with the Mg^{2+} or by impeding D94 interactions with the bridge.

As a control for the above experiment, the effects of A90 mutations on the Mg^{2+} requirement for DNA cleavage induced by 8-methyl-3'-(AM)P-dione (which does not require a metal ion for enzyme interactions) were determined. In contrast to results with ciprofloxacin, similar levels of

Mg^{2+} were required to achieve half-maximal and maximal cleavage with all three enzymes (Figure 3, right).

In other bacterial type II topoisomerases, mutations in bridge-anchoring residues that partially disrupt the water-metal ion bridge often restrict the variety of metal ions that can be used to form the bridge (21, 33). Therefore, we examined the ability of a second divalent metal ion, Mn^{2+}, to support ciprofloxacin activity against wild-type gyrase and enzymes with mutations at position 90 (Figure 4). With $GyrA^{A90S}$, which has a fully intact bridge, the level of ciprofloxacin-induced DNA cleavage was unaffected by the substitution of this metal ion for Mg^{2+}. However, with wild-type gyrase, which has a partially disrupted bridge, ciprofloxacin activity was decreased ~2-fold. Furthermore, with $GyrA^{A90V}$, which has a more severely disrupted bridge, the quinolone displayed no ability to enhance enzyme-mediated DNA cleavage in the presence of Mn^{2+}. Therefore, relative levels of resistance seen with enzymes containing mutations in bridge-anchoring residues can be altered by the metal ion used to support this interaction. A stronger water-metal ion bridge allows more latitude with metal ion requirements.

The water-metal ion bridge has been shown to play critical roles in mediating fluoroquinolone binding and positioning, but its predominant role appears to differ across species. With *B. anthracis* topoisomerase IV, it primarily acts as a binding contact (20, 21). However, with *E. coli* topoisomerase IV, it has little effect on drug affinity and is believed to properly position the drug in a manner that promotes DNA cleavage (33). Therefore, to determine whether the water-metal ion bridge plays a major role in drug-enzyme binding in *M. tuberculosis* gyrase, we used a competition approach and examined the effects of ciprofloxacin on DNA cleavage induced by 10 μM 8-methyl-3'-(AM)P-dione in two enzymes with impaired bridge function ($GyrA^{A90V}$ and $GyrA^{D94G}$). In an enzyme with optimal bridge function ($GyrA^{A90S}$), the fluoroquinolone and quinazolinedione display similar abilities to induce gyrase-mediated DNA cleavage and act with comparable potencies (see Figure 2 left, top and middle).

With both resistant mutant enzymes ($GyrA^{A90V}$ and $GyrA^{D94G}$), ciprofloxacin competed poorly against the bridge-independent quinazolinedione (Figure 5). Even at a 10-fold molar excess of the quinolone, levels of DNA cleavage decreased by only ~25%. This finding implies that impaired

bridge function decreases the affinity of ciprofloxacin for the enzyme at least an order of magnitude and strongly suggests that in *M. tuberculosis* gyrase the water-metal ion bridge plays a critical role in mediating quinolone binding.

Enhancing Fluoroquinolone Activity Against Wild-type and Resistant *M. tuberculosis* Gyrase by Modifying Substituents at C7 and C8. Previous studies (43, 44) have shown that fluoroquinolones containing a substituent at C8 (in particular, a methoxy group) display higher activity against *M. tuberculosis* and related organisms. However, the basis for the effects of C8 substitutions on fluoroquinolone activity against *M. tuberculosis* gyrase is not well understood. Therefore, we compared the activities of fluoroquinolones containing a C8–H, –methyl, or –methoxy group against the wild-type and resistant enzymes. Two parallel series were examined: one that contained the C7 piperazinyl ring of ciprofloxacin, and one that contained the C7 diazabicyclononyl ring of moxifloxacin.

The first set of experiments examined drug effects against wild-type gyrase. In general, the inclusion of a C8 substituent enhanced quinolone activity (Figure 6, top left). For the ciprofloxacin-based series, the compound with a C8 methoxy group generated the highest level of DNA cleavage activity. Compared to ciprofloxacin, 8-methoxy-cipro induced ~50% more cleavage at 100 μM drug and displayed a potency that was ~2-fold higher (based on the drug concentration required to induce 50% of the cleavage generated at 100 μM drug). The presence of a C8 methyl group enhanced DNA cleavage, but to a lesser extent than did the methoxy group.

A more dramatic effect was seen when the C8 methoxy group of moxifloxacin was replaced with a methyl group. Compared to moxifloxacin (the fluoroquinolone most commonly used to treat tuberculosis) (2, 4-6), 8-methyl-moxi induced ~2-fold more cleavage at 100 μM drug and was ~2-fold more potent. Furthermore, only 10 μM 8-methyl-moxi was required to induce the same level of scission (~30%) as was seen with 100 μM moxifloxacin. In contrast, 8-H-moxi displayed an activity similar to that of moxifloxacin.

The second set of experiments examined the effects of the C8 substituent on fluoroquinolone activity against the resistant $GyrA^{A90V}$ and $GyrA^{D94G}$ mutant enzymes (Figure 6, top right and bottom left, respectively). When the function of the water-metal ion bridge was disrupted, the C8

substituent had a much greater influence on drug activity. Drugs lacking a C8 substituent (ciprofloxacin and 8-H-moxi) showed little activity against either fluoroquinolone-resistant enzyme. However, in the presence of either a C8 methyl or methoxy substituent, high levels of activity were maintained. To this point, 8-methyl-moxi displayed nearly wild-type activity against $GyrA^{A90V}$. Moreover, even though its activity against $GyrA^{D94G}$ was decreased, 8-methyl-moxi still induced higher levels of cleavage than did moxifloxacin with wild-type gyrase. Representative gels showing the effects of moxifloxacin and 8-methyl-moxi on DNA cleavage mediated by the mutant $GyrA^{D94G}$ enzyme are shown in Supplemental Figure S2.

Some fluoroquinolones and related compounds that display high activity against resistant bacterial type II topoisomerases cross-react with human topoisomerase IIα, excluding them from clinical development as antibacterial drugs. For example, CP-115,955 induces higher levels of cleavage with the human enzyme than does etoposide, a commonly prescribed anticancer drug (45, 46) (Figure 6, bottom right). Notably, none of the ciprofloxacin- or moxifloxacin-based compounds employed in this study displayed significant activity against human topoisomerase IIα.

To further understand the contributions of the C7 and C8 substituents to quinolone activity, we determined the abilities of the two least effective compounds (ciprofloxacin and 8-H-moxi) to compete with the two most effective drugs (8-methoxy-cipro and 8-methyl-moxi) (Figure 7, left and right, respectively). The $GyrA^{A90V}$ and $GyrA^{D94G}$ mutant enzymes were used so that the contributions of the C7 and C8 groups would not be obscured by the water-metal ion bridge. A representative gel showing the effects of ciprofloxacin and 8-H-moxi on DNA cleavage mediated by the $GyrA^{D94G}$ mutant gyrase in the presence of 50 μM 8-methoxy-cipro is shown in Supplemental Figure S3. Three observations were noted. First, the concentrations of ciprofloxacin and 8-H-moxi required to compete out 50% of the DNA cleavage induced by 50 μM 8-methyl-cipro or 8-methyl-moxi were 100 μM or higher. This finding (which is consistent with the potency data discussed for Figure 6) indicates that the C8-H derivatives display a decreased affinity for the enzymes as compared to 8-methoxy-cipro and 8-methyl-moxi. Thus, a C8 group appears to contribute to drug binding within the enzyme-DNA cleavage complex. Second, compounds bearing a C7 diazabicyclononyl group (as found in moxifloxacin) competed better than those with a C7

piperazinyl substituent (as found in ciprofloxacin), suggesting that moxifloxacin- as opposed to ciprofloxacin-based analogs interact more tightly with *M. tuberculosis* gyrase. Third, each compound competed less effectively against 8-methyl-moxi than against 8-methoxy-cipro, indicating that 8-methyl-moxi interacts more tightly with the enzyme. This finding is consistent with the observation that 8-methyl-moxi induced higher levels of DNA cleavage with all of the enzymes tested than did the other fluoroquinolones in these two series (see Figure 6).

Finally, to further examine the contributions of the C7 and C8 substituents to quinolone action, we determined the persistence of cleavage complexes formed in the presence of ciprofloxacin, moxifloxacin, 8-methoxy-cipro, and 8-methyl-moxi (Figure 8). Moxifloxacin induced more stable cleavage complexes than ciprofloxacin with all three enzymes. This finding is consistent with binding studies (47) suggesting that moxifloxacin binds more tightly than ciprofloxacin to *M. tuberculosis* gyrase. Furthermore, consistent with the competition experiments, compounds containing the C7 diazabicyclononyl group of moxifloxacin induced cleavage complexes that were more stable than those formed with the C7 piperazinyl group of ciprofloxacin with both the wild-type and resistant enzymes. Lastly, in all cases, 8-methyl-moxi induced the most stable cleavage complexes. Once again, this finding correlates with the high activity of 8-methyl-moxi.

Summary. As fluoroquinolones become more important for the treatment of tuberculosis and resistance becomes more prevalent, there is a critical need to understand the binding interactions and mechanistic details of quinolone-based agents with *M. tuberculosis* gyrase in order to develop new agents with high activity against wild-type and resistant disease. Thus, we analyzed interactions between quinolone-based agents and wild-type *M. tuberculosis* gyrase and resistant mutants. The interaction of current fluoroquinolones with gyrase is governed predominately by a critical water-metal ion bridge. However, in contrast to most bacterial type II enzymes, *M. tuberculosis* gyrase uses only one amino acid to anchor the bridge. The most common resistance-conferring mutations in gyrase disrupt the bridge interaction between fluoroquinolones and the enzyme. When bridge function is compromised, resistance can be overcome, at least in part, by the introduction of specific groups at the C7 and C8 positions. By dissecting fluoroquinolone-enzyme interactions, we determined that an 8-methyl derivative of moxifloxacin induces high levels of

stable cleavage complexes with wild-type and common fluoroquinolone-resistant mutant enzymes. This chemical biology approach to understanding the basis for fluoroquinolone-enzyme interactions has the potential to guide the future development of novel agents with improved activity against tuberculosis.

Methods

Materials and Enzymes. Ciprofloxacin and moxifloxacin were obtained from LKT Laboratories. 8-Methyl-cipro, 8-methoxy-cipro, 8-H-moxi, 8-methyl-moxi, 8-H-3'-(AM)P-FQ, 8-H-3'-(AM)P-dione, 8-methyl-3'-(AM)P-FQ, and 8-methyl-3'-(AM)P-dione were synthesized as reported previously (32). Ciprofloxacin-based compounds were stored at -20 °C as 40 mM stock solutions in 0.1 N NaOH and diluted five-fold with 10 mM Tris–HCl (pH 7.9) immediately prior to use. All other compounds were stored at 4 °C as 20 mM stock solutions in 100% DMSO. Supplementary Table S1 contains the full chemical, library, and abbreviated names for the compounds used in this study. Other chemicals were analytical reagent grade.

The coding regions for residues 2-675 of GyrB and 2-838 of GyrA from *M. tuberculosis* were amplified from genomic DNA (American Type Culture Collection strain H37Rv) and individually cloned into a pET-28b derivative containing an N-terminal, tobacco etch virus (TEV) protease-cleavable hexahistidine tag. Mutant GyrA vectors were generated by QuikChange (Agilent). Proteins were overexpressed in *E. coli* strain Rosetta 2 pLysS (EMD Millipore) by growing cells at 30 °C until log phase, then inducing with 1 mM isopropyl-β-D-thiogalactopyranoside for 3 h. Cells were harvested by centrifugation and resuspended in buffer A [20 mM Tris–HCl (pH 7.9), 500 mM NaCl, 5 mM imidazole, and 10% glycerol with protease inhibitors], then frozen drop wise in liquid nitrogen.

Cells were sonicated and centrifuged, and the clarified lysate was passed over a HisTrap HP column (GE Healthcare). His-tagged protein was eluted with buffer B [20 mM Tris–HCl (pH 7.9), 500 mM NaCl, 250 mM imidazole, and 10% glycerol with protease inhibitors], then concentrated and exchanged into buffer A overnight at 4 °C, in the presence of His-tagged TEV protease. This mixture was passed over a HisTrap HP column, and the flow-through was collected, concentrated,

and run over an S-300 gel filtration column (GE Healthcare) in buffer C [50 mM Tris–HCl (pH 7.9), 500 mM KCl, 2 mM β-mercaptoethanol, and 10% glycerol]. Peak fractions were pooled, concentrated, and diluted into a high-glycerol variant of buffer C, so that the final glycerol concentration reached 30% prior to storage at -80 °C.

Human topoisomerase IIα was expressed in yeast and purified as described by Kingma et al. (48).

Negatively supercoiled pBR322 plasmid DNA was prepared from *E. coli* using a Plasmid Mega Kit (Qiagen) as described by the manufacturer. Relaxed pBR322 plasmid DNA was generated by treatment with topoisomerase I for 30 min as previously described (49), followed by phenol-chloroform-isoamyl alcohol extraction, ethanol precipitation, and resuspension in 5 mM Tris-HCl (pH 8.5) and 500 μM EDTA.

DNA Supercoiling. DNA supercoiling reactions (20 μL) contained 25 nM wild-type or mutant gyrase and 5 nM relaxed pBR322 in reaction buffer [10 mM Tris–HCl (pH 7.5), 40 mM KCl, 0.1 mg/mL BSA, 6 mM $MgCl_2$, 10% (v/v) glycerol, and 0.5 mM DTT] supplemented with 1 mM ATP and were incubated at 37 °C. DNA supercoiling was stopped at times from 0–45 min by the addition of 3 μL of 0.77% SDS and 77.5 mM EDTA. Samples were mixed with 2 μL of agarose gel loading buffer [60% sucrose, 10 mM Tris–HCl (pH 7.9), 0.5% bromophenol blue, and 0.5% xylene cyanol FF], heated at 45 °C for 5 min, and subjected to electrophoresis in 1% agarose gels in 100 mM Tris–borate (pH 8.3) and 2 mM EDTA. Gels were stained with 0.75 μg/mL ethidium bromide for 30 min. DNA bands were visualized with medium-range ultraviolet light and quantified using an Alpha Innotech digital imaging system.

DNA Cleavage. DNA cleavage reactions were carried out using the procedure of Fortune and Osheroff as adapted by Aldred et al. (20, 50). Reactions with the bacterial enzyme contained 100 nM wild-type or mutant gyrase and 10 nM negatively supercoiled pBR322 in a total of 20 μL of reaction buffer. Reactions with the human enzyme contained 110 nM human topoisomerase IIα and 10 nM negatively supercoiled pBR322 in a total of 20 μL of 10 mM Tris–HCl (pH 7.9), 5 mM $MgCl_2$, 100 mM KCl, 100 μM EDTA, 25 μM dithiothreitol, and 2.5% (v/v) glycerol. All reaction mixtures were incubated at 37 °C for 10 min, and enzyme-DNA cleavage complexes were trapped

by the addition of 2 µL of 5% SDS followed by 2 µL of 250 mM EDTA (pH 8.0). Proteinase K (2 µL of a 0.8 mg/mL solution) was added, and samples were incubated at 45 °C for 45 min to digest the enzyme. Samples were mixed with 2 µL of agarose gel loading buffer, heated at 45 °C for 5 min, and subjected to electrophoresis in 1% agarose gels in 40 mM Tris–acetate (pH 8.3) and 2 mM EDTA containing 0.5 µg/mL ethidium bromide. DNA bands were visualized as described above. DNA cleavage was monitored by the conversion of supercoiled plasmid to linear molecules.

Assays that monitored gyrase-mediated DNA cleavage in the absence of drugs substituted 6 mM $CaCl_2$ for 6 mM $MgCl_2$ in the reaction buffer. Assays that assessed DNA cleavage in the presence of drugs contained 0–100 µM compound. In some reactions, the concentration dependence of $MgCl_2$ was examined or the divalent metal ion was replaced with 2.5 mM $MnCl_2$.

For assays that monitored competition between two drugs, the compounds were added simultaneously to reaction mixtures, and the final concentrations of the compounds are indicated. In these competition assays, the level of cleavage seen with the corresponding concentration of the competing drug (in the absence of the drug held at a constant concentration) was used as a baseline and was subtracted from the cleavage level seen in the presence of both compounds.

Persistence of Gyrase-DNA Cleavage Complexes. The persistence of gyrase-DNA cleavage complexes established in the presence of drugs was determined using the procedure of Gentry et al. as adapted by Aldred et al. (20, 51). Initial reaction mixtures contained 500 nM wild-type or mutant gyrase, 50 nM DNA, and 100 µM ciprofloxacin, 50 µM 8-methoxy-cipro, 50 µM moxifloxacin, or 10 µM 8-methyl-moxi in a total of 20 µL of reaction buffer. Quinolone concentrations that yielded similar levels of DNA cleavage were used. Reaction mixtures were incubated at 37 ºC for 10 min and then diluted 20–fold with reaction buffer warmed to 37 ºC. Samples (20 µL) were removed at times ranging from 0–60 min for the mutant enzymes or 0–180 min for the wild-type enzyme, and DNA cleavage was stopped with 2 µL of 5% SDS followed by 2 µL of 250 mM EDTA (pH 8.0). Samples were digested with proteinase K and processed as described above for DNA cleavage assays. Levels of DNA cleavage were set to 100% at time zero, and the persistence of cleavage complexes was determined by the loss of the linear reaction product over time.

ACKNOWLEDGEMENTS

K.J.A. was a trainee under grant T32 CA09582 from the National Institutes of Health. T.R.B. was supported by a European Molecular Biology Organization Long-Term Fellowship. This work was supported by United States Veterans Administration Merit Review award I01 Bx002198 (to N.O.) and National Institutes of Health research grants R01 AI87671 (to R.J.K.), R01 CA077373 (to J.M.B.), and R01 GM033944 (to N.O.). We are grateful to H. Schwanz and G. Li for the preparation of compounds and to M. Pendleton and R. Ashley for critical reading of the manuscript.

REFERENCES

1. World Health Organization (2014) Tuberculosis. Fact Sheet No 104. http://www.who.int/mediacentre/factsheets/fs104/en/. Accessed: July 21, 2014.
2. World Health Organization. (2010) *Treatment of tuberculosis: guidelines - 4th ed.* (WHO Press, Geneva).
3. TB CARE I. (2014) *International Standards for Tuberculosis Care, Edition 3* (TB CARE I, The Hague).
4. American Thoracic Society, Centers for Disease Control and Prevention, Infectious Diseases Society of America (2003) Treatment of tuberculosis. *MMWR Recomm Rep* 52:1-77.
5. World Health Organization. (2011) *Guidelines for the programmatic management of drug-resistant tuberculosis* (WHO Press, Geneva).
6. TB Alliance Interactive Portfolio (PaMZ. http://wwwtballianceorg/portfolio/regimen/pamz.
7. Hooper DC (1998) Clinical applications of quinolones. *Biochim Biophys Acta* 1400(1-3):45-61.
8. Hooper DC (2001) Mechanisms of action of antimicrobials: focus on fluoroquinolones. *Clin Infect Dis* 32 Suppl. 1:S9-S15.
9. Andriole VT (2005) The quinolones: past, present, and future. *Clin Infect Dis* 41 Suppl. 2:S113-119.
10. Drlica K, et al. (2009) Quinolones: action and resistance updated. *Curr Top Med Chem* 9(11):981-998.
11. Pommier Y, Leo E, Zhang H, Marchand C (2010) DNA topoisomerases and their poisoning by anticancer and antibacterial drugs. *Chem Biol* 17(5):421-433.
12. Aldred KJ, Kerns RJ, Osheroff N (2014) Mechanism of quinolone action and resistance. *Biochemistry* 53(10):1565-1574.
13. Anderson VE, Osheroff N (2001) Type II topoisomerases as targets for quinolone antibacterials: turning Dr. Jekyll into Mr. Hyde. *Curr Pharm Des* 7(5):337-353.

14. Drlica K, Malik M, Kerns RJ, Zhao X (2008) Quinolone-mediated bacterial death. *Antimicrob Agents Chemother* 52(2):385-392.
15. Levine C, Hiasa H, Marians KJ (1998) DNA gyrase and topoisomerase IV: biochemical activities, physiological roles during chromosome replication, and drug sensitivities. *Biochim Biophys Acta* 1400(1-3):29-43.
16. Champoux JJ (2001) DNA topoisomerases: structure, function, and mechanism. *Annu Rev Biochem* 70:369-413.
17. Cole ST, et al. (1998) Deciphering the biology of *Mycobacterium tuberculosis* from the complete genome sequence. *Nature* 393(6685):537-544.
18. Aubry A, Fisher LM, Jarlier V, Cambau E (2006) First functional characterization of a singly expressed bacterial type II topoisomerase: the enzyme from *Mycobacterium tuberculosis*. *Biochem Biophys Res Commun* 348(1):158-165.
19. Wohlkonig A, et al. (2010) Structural basis of quinolone inhibition of type IIA topoisomerases and target-mediated resistance. *Nat Struct Mol Biol* 17(9):1152-1153.
20. Aldred KJ, et al. (2012) Drug interactions with *Bacillus anthracis* topoisomerase IV: biochemical basis for quinolone action and resistance. *Biochemistry* 51(1):370-381.
21. Aldred KJ, McPherson SA, Turnbough CL, Jr., Kerns RJ, Osheroff N (2013) Topoisomerase IV-quinolone interactions are mediated through a water-metal ion bridge: mechanistic basis of quinolone resistance. *Nucleic Acids Res* 41(8):4628-4639.
22. Drlica K, Zhao X (1997) DNA gyrase, topoisomerase IV, and the 4-quinolones. *Microbiol Mol Biol Rev* 61(3):377-392.
23. Li Z, et al. (1998) Alteration in the GyrA subunit of DNA gyrase and the ParC subunit of DNA topoisomerase IV in quinolone-resistant clinical isolates of *Staphylococcus epidermidis*. *Antimicrob Agents Chemother* 42(12):3293-3295.
24. Hooper DC (1999) Mode of action of fluoroquinolones. *Drugs* 58 Suppl. 2:6-10.

25. Price LB, et al. (2003) *In vitro* selection and characterization of *Bacillus anthracis* mutants with high-level resistance to ciprofloxacin. *Antimicrob Agents Chemother* 47(7):2362-2365.
26. Morgan-Linnell SK, Becnel Boyd L, Steffen D, Zechiedrich L (2009) Mechanisms accounting for fluoroquinolone resistance in *Escherichia coli* clinical isolates. *Antimicrob Agents Chemother* 53(1):235-241.
27. Bansal S, Tandon V (2011) Contribution of mutations in DNA gyrase and topoisomerase IV genes to ciprofloxacin resistance in *Escherichia coli* clinical isolates. *Int J Antimicrob Agents* 37(3):253-255.
28. Maruri F, et al. (2012) A systematic review of gyrase mutations associated with fluoroquinolone-resistant *Mycobacterium tuberculosis* and a proposed gyrase numbering system. *J Antimicrob Chemother* 67(4):819-831.
29. Grossman RF, Hsueh PR, Gillespie SH, Blasi F (2014) Community-acquired pneumonia and tuberculosis: differential diagnosis and the use of fluoroquinolones. *Int J Infect Dis* 18:14-21.
30. Long R, et al. (2009) Empirical treatment of community-acquired pneumonia and the development of fluoroquinolone-resistant tuberculosis. *Clin Infect Dis* 48(10):1354-1360.
31. Devasia RA, et al. (2009) Fluoroquinolone resistance in *Mycobacterium tuberculosis*: the effect of duration and timing of fluoroquinolone exposure. *Am J Respir Crit Care Med* 180(4):365-370.
32. Aldred KJ, et al. (2013) Overcoming target-mediated quinolone resistance in topoisomerase IV by introducing metal-ion-independent drug-enzyme interactions. *ACS Chem Biol* 8(12):2660-2668.
33. Aldred KJ, et al. (2014) Role of the water-metal ion bridge in mediating interactions between quinolones and *Escherichia coli* topoisomerase IV. *Biochemistry* 53(34):5558-5567.

34. Blower TR, Williamson BH, Kerns RJ, Berger JM (2016) Crystal structure and stability of gyrase-fluoroquinolone cleaved complexes from *M. tuberculosis*. *Proc Natl Acad Sci U S A*, in press.
35. Camus JC, Pryor MJ, Medigue C, Cole ST (2002) Re-annotation of the genome sequence of *Mycobacterium tuberculosis* H37Rv. *Microbiology* 148(Pt 10):2967-2973.
36. Xu C, Kreiswirth BN, Sreevatsan S, Musser JM, Drlica K (1996) Fluoroquinolone resistance associated with specific gyrase mutations in clinical isolates of multidrug-resistant *Mycobacterium tuberculosis*. *J Infect Dis* 174(5):1127-1130.
37. Aubry A, et al. (2006) Novel gyrase mutations in quinolone-resistant and -hypersusceptible clinical isolates of *Mycobacterium tuberculosis*: functional analysis of mutant enzymes. *Antimicrob Agents Chemother* 50(1):104-112.
38. Tran TP, et al. (2007) Structure-activity relationships of 3-aminoquinazolinediones, a new class of bacterial type-2 topoisomerase (DNA gyrase and topo IV) inhibitors. *Bioorg Med Chem Lett* 17(5):1312-1320.
39. German N, Malik M, Rosen JD, Drlica K, Kerns RJ (2008) Use of gyrase resistance mutants to guide selection of 8-methoxy-quinazoline-2,4-diones. *Antimicrob Agents Chemother* 52(11):3915-3921.
40. Pan XS, Gould KA, Fisher LM (2009) Probing the differential interactions of quinazolinedione PD 0305970 and quinolones with gyrase and topoisomerase IV. *Antimicrob Agents Chemother* 53(9):3822-3831.
41. Oppegard LM, et al. (2010) Comparison of *in vitro* activities of fluoroquinolone-like 2,4- and 1,3-diones. *Antimicrob Agents Chemother* 54(7):3011-3014.
42. Malik M, et al. (2011) Fluoroquinolone and quinazolinedione activities against wild-type and gyrase mutant strains of *Mycobacterium smegmatis*. *Antimicrob Agents Chemother* 55(5):2335-2343.

43. Dong Y, Xu C, Zhao X, Domagala J, Drlica K (1998) Fluoroquinolone action against mycobacteria: effects of C-8 substituents on growth, survival, and resistance. *Antimicrob Agents Chemother* 42(11):2978-2984.
44. Zhao BY, Pine R, Domagala J, Drlica K (1999) Fluoroquinolone action against clinical isolates of *Mycobacterium tuberculosis*: effects of a C-8 methoxyl group on survival in liquid media and in human macrophages. *Antimicrob Agents Chemother* 43(3):661-666.
45. Hande KR (1998) Etoposide: four decades of development of a topoisomerase II inhibitor. *Eur J Cancer* 34(10):1514-1521.
46. Baldwin EL, Osheroff N (2005) Etoposide, topoisomerase II and cancer. *Curr Med Chem Anticancer Agents* 5(4):363-372.
47. Kumar R, Madhumathi BS, Nagaraja V (2014) Molecular basis for the differential quinolone susceptibility of mycobacterial DNA gyrase. *Antimicrob Agents Chemother* 58(4):2013-2020.
48. Kingma PS, Greider CA, Osheroff N (1997) Spontaneous DNA lesions poison human topoisomerase IIα and stimulate cleavage proximal to leukemic 11q23 chromosomal breakpoints. *Biochemistry* 36(20):5934-5939.
49. Fortune JM, Velea L, Graves DE, Osheroff N (1999) DNA topoisomerases as targets for the anticancer drug TAS-103: DNA interactions and topoisomerase catalytic inhibition. *Biochemistry* 38(47):15580-15586.
50. Fortune JM, Osheroff N (1998) Merbarone inhibits the catalytic activity of human topoisomerase IIα by blocking DNA cleavage. *J Biol Chem* 273(28):17643-17650.
51. Gentry AC, et al. (2011) Interactions between the etoposide derivative F14512 and human type II topoisomerases: implications for the C4 spermine moiety in promoting enzyme-mediated DNA cleavage. *Biochemistry* 50(15):3240-3249.

FIGURE LEGENDS

Figure 1. Catalytic and DNA cleavage activities of wild-type and mutant *M. tuberculosis* gyrase in the absence of drugs. The ability of wild-type (WT, black), GyrA^{A90S} (A90S, blue), GyrA^{A90V} (A90V, red), GyrA^{D94H} (D94H, green), and GyrA^{D94G} (D94G, yellow) to supercoil relaxed pBR322 plasmid DNA is shown on the left. Gels are representative of three independent experiments. The positions of negatively supercoiled [(-)SC] and relaxed (Rel) DNA controls are indicated. The ability of the enzymes to cleave negatively supercoiled pBR322 plasmid DNA is shown on the right. Error bars represent the standard deviation of at least three independent experiments.

Figure 2. Drug-induced DNA cleavage mediated by wild-type and mutant *M. tuberculosis* gyrase. The ability of wild-type (WT, black), GyrA^{A90S} (A90S, blue), GyrA^{A90V} (A90V, red), GyrA^{D94H} (D94H, green), and GyrA^{D94G} (D94G, yellow) to mediate DNA cleavage in the presence of the clinically used fluoroquinolones ciprofloxacin and moxifloxacin (top left and right, respectively), the experimental quinazolinediones 8-methyl-3'-(AM)P-dione and 8-H-3'-(AM)P-dione (middle left and bottom left, respectively), and the experimental fluoroquinolones 8-methyl-3'-(AM)P-FQ and 8-H-3'-(AM)P-FQ (middle right and bottom right, respectively) is shown. Compound structures are shown in or above their respective panels. Error bars represent the standard deviation of at least three independent experiments.

Figure 3. Effects of Mg^{2+} concentration on DNA cleavage mediated by wild-type and mutant *M. tuberculosis* gyrase. Results are shown for 10 μM ciprofloxacin (left) and 10 μM 8-methyl-3'-(AM)P-dione (right) with wild-type (WT, black), GyrA^{A90S} (A90S, blue), and GyrA^{A90V} (A90V, red). DNA cleavage for each drug-enzyme pair was normalized to 100% at 6 mM Mg^{2+} to facilitate direct comparisons. Error bars represent the standard deviation of at least three independent experiments.

Figure 4. Effects of Mn^{2+} on drug-induced DNA cleavage mediated by wild-type and mutant *M. tuberculosis* gyrase. Results are shown for cleavage mediated by wild-type (WT, black), GyrA^{A90S} (A90S, blue), and GyrA^{A90V} (A90V, red) in the presence of ciprofloxacin. Assays included 2.5 mM Mn^{2+}, the concentration that yielded maximal enzyme activity, instead of Mg^{2+}. Error bars represent

the standard deviation of at least three independent experiments.

Figure 5. Ability of ciprofloxacin to compete out DNA cleavage induced by 10 μM 8-methyl-3'-(AM)P-dione with mutant *M. tuberculosis* gyrase. Results are shown for $GyrA^{A90V}$ (A90V, red) and $GyrA^{D94G}$ (D94G, yellow). Both drugs were added to reaction mixtures simultaneously. The low level of cleavage seen in the presence of ciprofloxacin alone was used as a baseline and was subtracted from DNA scission observed in the presence of both drugs. The level of DNA cleavage observed in the presence of the quinazolinedione alone was set to 1.0 to facilitate direct comparisons. Error bars represent the standard deviation of at least three independent experiments.

Figure 6. Effects of ciprofloxacin- and moxifloxacin-based fluoroquinolones on DNA cleavage mediated by wild-type and mutant *M. tuberculosis* gyrase and human topoisomerase IIα. The ability of wild-type (WT, top left), $GyrA^{A90V}$ (A90V, top right), and $GyrA^{D94G}$ (D94G, bottom left) gyrase and human topoisomerase IIα (hTIIα, bottom right) to cleave DNA in the presence of fluoroquinolones containing a C8–H (black), –methyl (blue), or –methoxy (red) group and a C7 piperazinyl (closed) or diazabicyclononyl (open) group is shown. For human topoisomerase IIα, DNA cleavage levels induced by the enzyme in the presence of CP-115,955 or etoposide (dashed lines) are shown for comparison. These latter data are from Aldred et al. (32). The ciprofloxacin and moxifloxacin fluoroquinolone cores are shown at the top. Error bars represent the standard deviation of at least three independent experiments.

Figure 7. Ability of fluoroquinolones with a C8-H to compete out DNA cleavage induced by 50 μM 8-methoxy-cipro or 8-methyl-moxi with mutant *M. tuberculosis* gyrase. Results are shown for $GyrA^{A90V}$ (A90V, black) and $GyrA^{D94G}$ (D94G, blue). Ciprofloxacin (Cipro, closed) or 8-H-moxi (open) and 8-methoxy-cipro (left) or 8-methyl-moxi (right) were added to reaction mixtures simultaneously. The low level of cleavage seen in the presence of the C8-H fluoroquinolones alone was used as a baseline and was subtracted from the DNA scission observed in the presence of both drugs. The level of DNA cleavage observed in the presence of 8-methoxy-cipro or 8-methyl-moxi alone was set to 1.0 to facilitate direct comparisons. Error bars represent the standard deviation of at

least three independent experiments.

Figure 8. Effects of fluoroquinolones on the persistence of cleavage complexes formed by wild-type and mutant *M. tuberculosis* gyrase. The stability of ternary enzyme-drug-DNA cleavage complexes formed with wild-type (WT, left), $GyrA^{A90V}$ (A90V, middle), and $GyrA^{D94G}$ (D94G, right) was determined in the presence of 100 µM ciprofloxacin (Cipro, black), 50 µM moxifloxacin (Moxi, blue), 50 µM 8-methoxy-cipro (red), or 10 µM 8-methyl-moxi (yellow). The data table (inset, middle) lists the $t_{1/2}$ of DNA cleavage complexes formed with each drug-enzyme combination. Initial DNA cleavage-religation reactions were allowed to come to equilibrium and were then diluted 20-fold with reaction buffer. Levels of DNA cleavage at time zero were set to 100%. Error bars represent the standard deviation of at least three independent experiments.

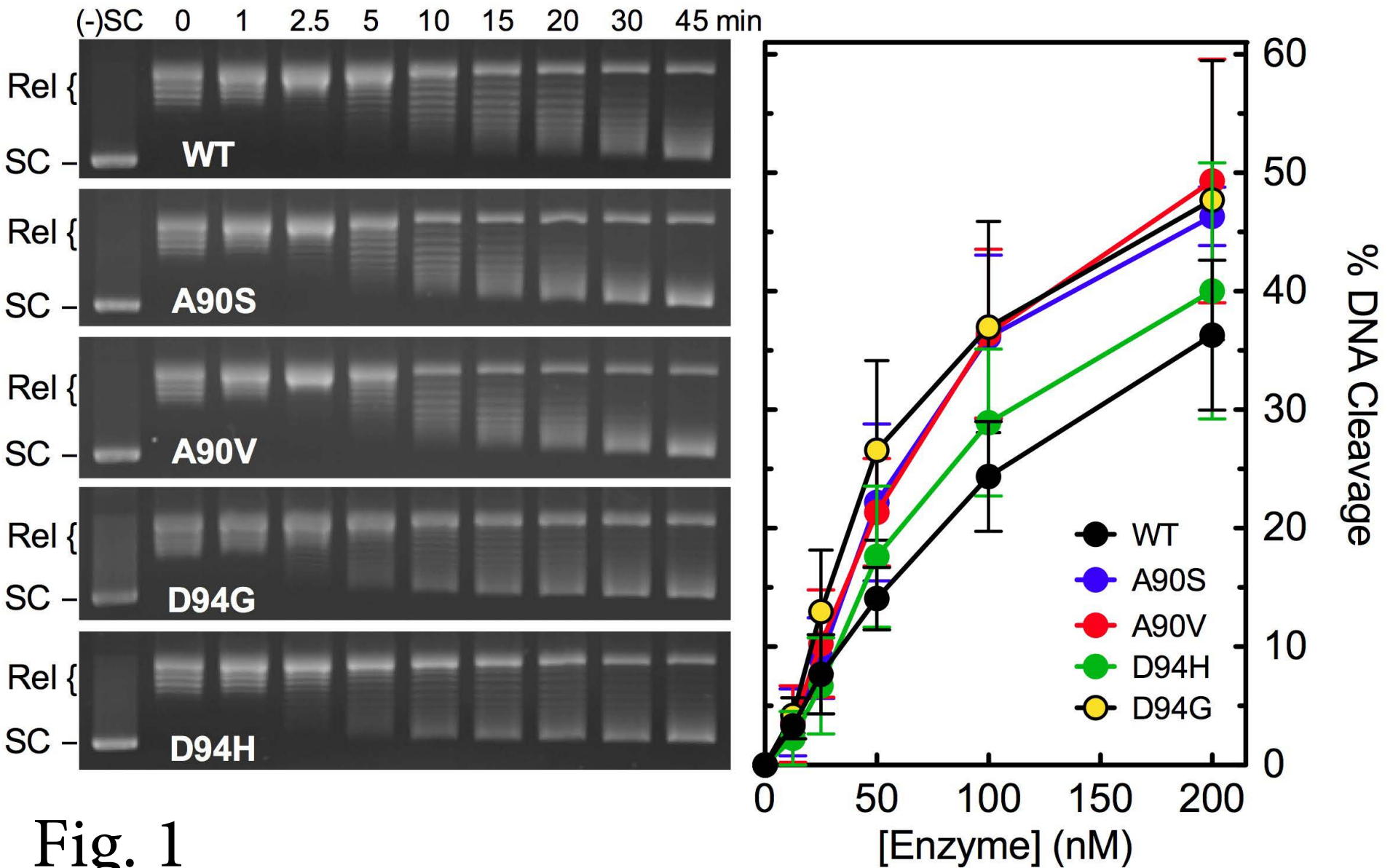
(-)SC 0 1 2.5 5 10 15 20 30 45 min
Rel {
SC –
WT
A90S
A90V
D94G
D94H
60
50
40
30
20
10
0
% DNA Cleavage
0 50 100 150 200
[Enzyme] (nM)
WT
A90S
A90V
D94H
D94G

Fig. 1

Fig. 2

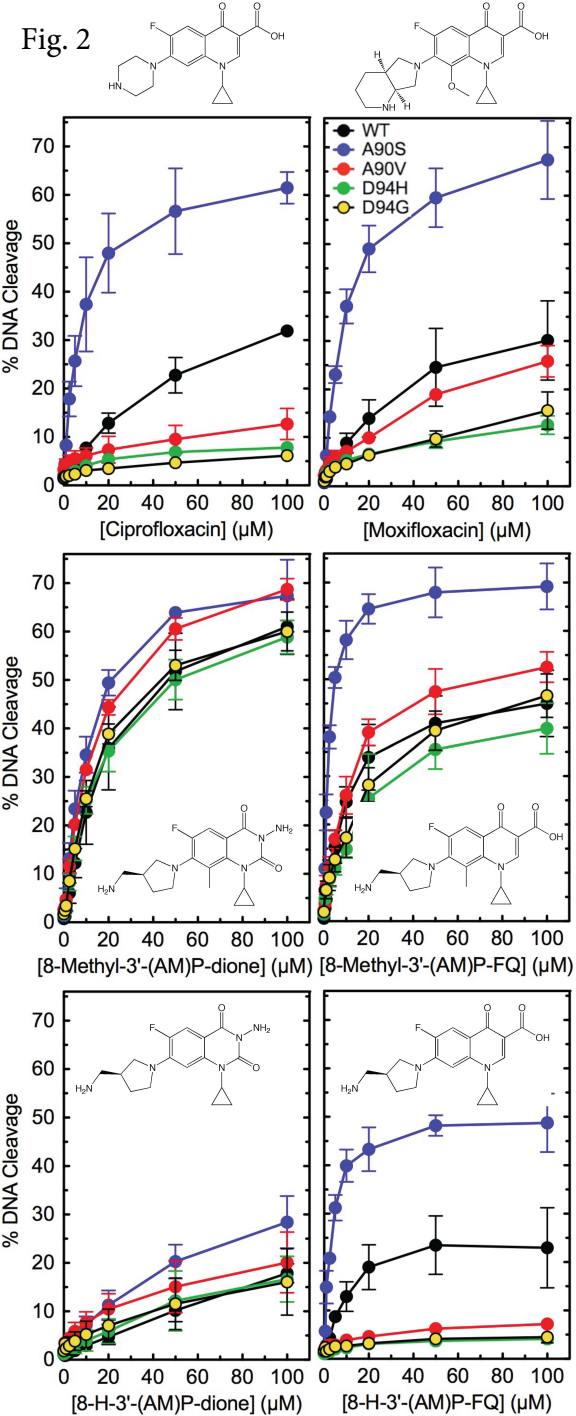
WT
A90S
A90V
D94H
D94G
% DNA Cleavage
[Ciprofloxacin] (μM)
[Moxifloxacin] (μM)
[8-Methyl-3'-(AM)P-dione] (μM)
[8-Methyl-3'-(AM)P-FQ] (μM)
[8-H-3'-(AM)P-dione] (μM)
[8-H-3'-(AM)P-FQ] (μM)

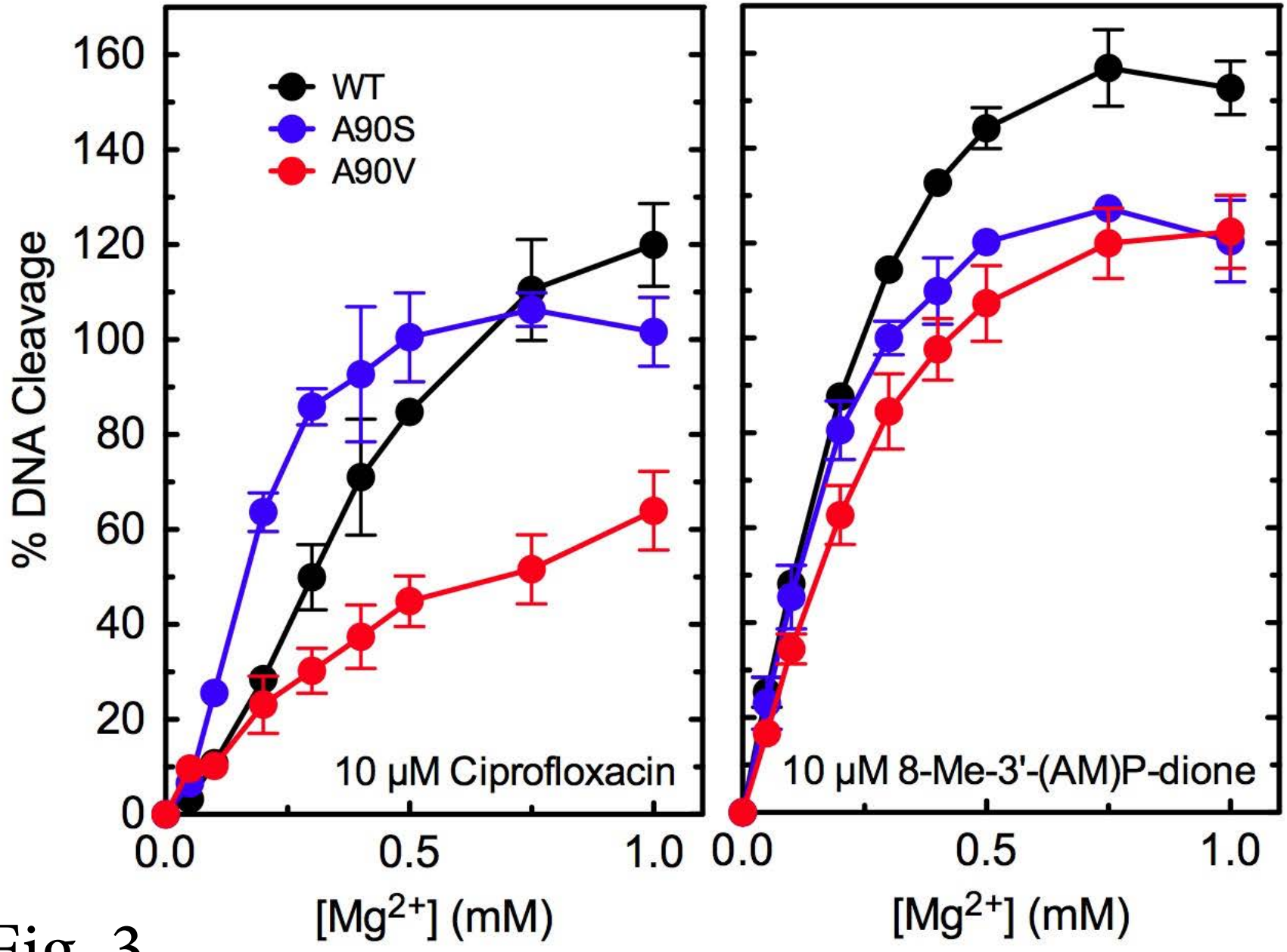
% DNA Cleavage
160
140
120
100
80
60
40
20
0
WT
A90S
A90V
10 μM Ciprofloxacin
0.0
0.5
1.0
[Mg2+] (mM)
10 μM 8-Me-3'-(AM)P-dione
0.0
0.5
1.0
[Mg2+] (mM)

Fig. 3

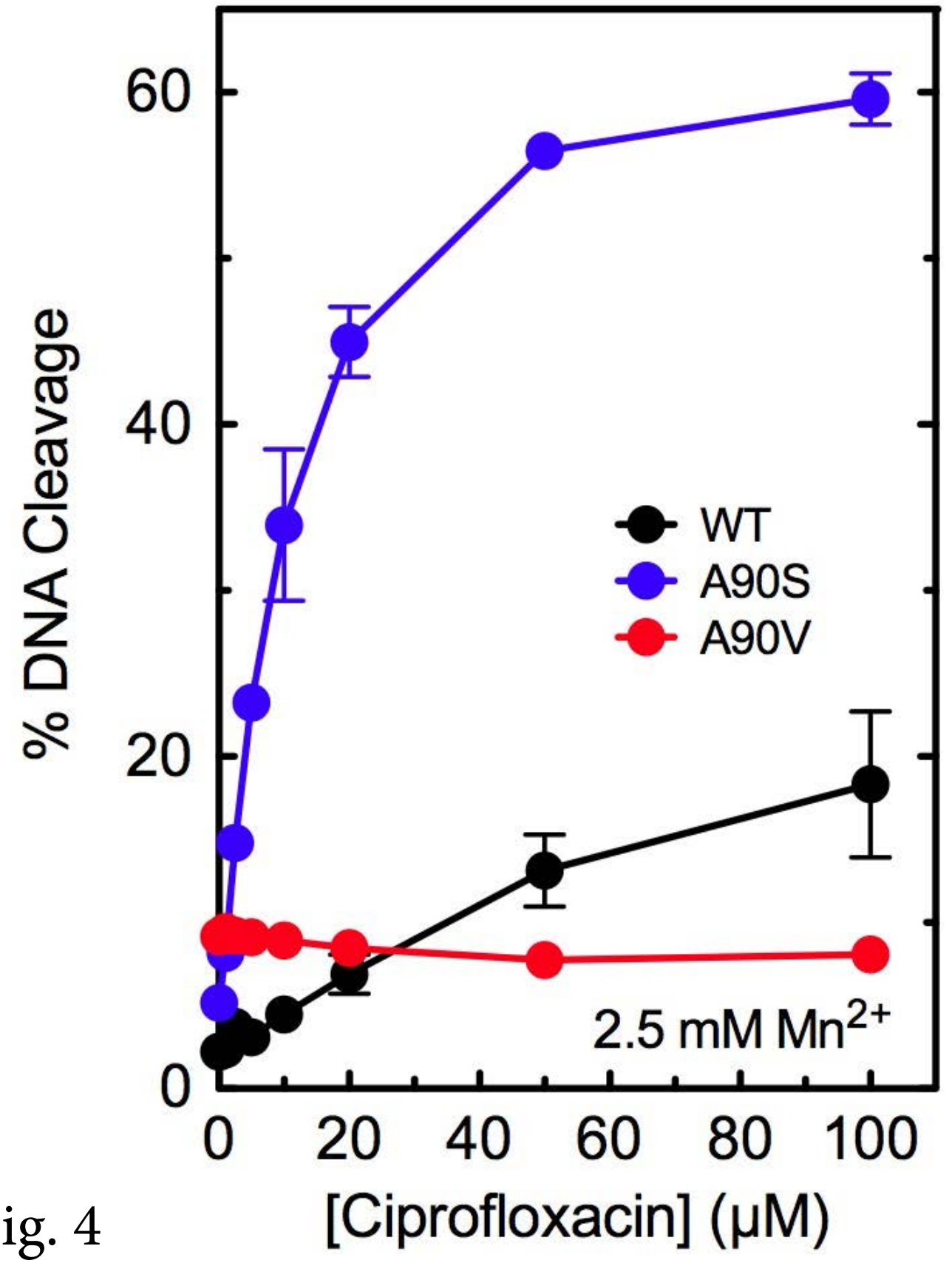
% DNA Cleavage
60
40
20
0
0
20
40
60
80
100
[Ciprofloxacin] (μM)
WT
A90S
A90V
2.5 mM Mn2+

Fig. 4

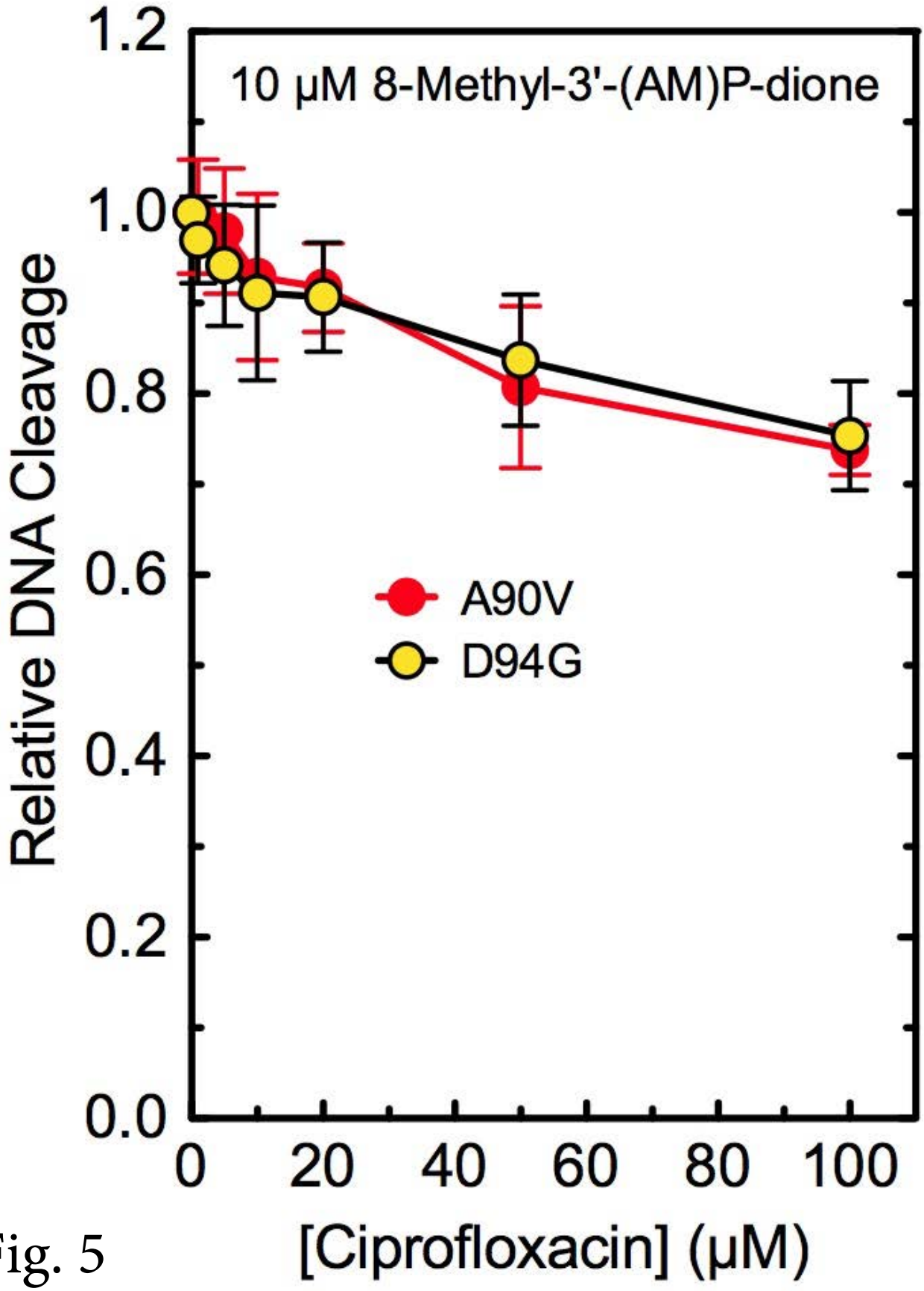
10 μM 8-Methyl-3'-(AM)P-dione
Relative DNA Cleavage
1.2
1.0
0.8
0.6
0.4
0.2
0.0
A90V
D94G
0
20
40
60
80
100
[Ciprofloxacin] (μM)

Fig. 5

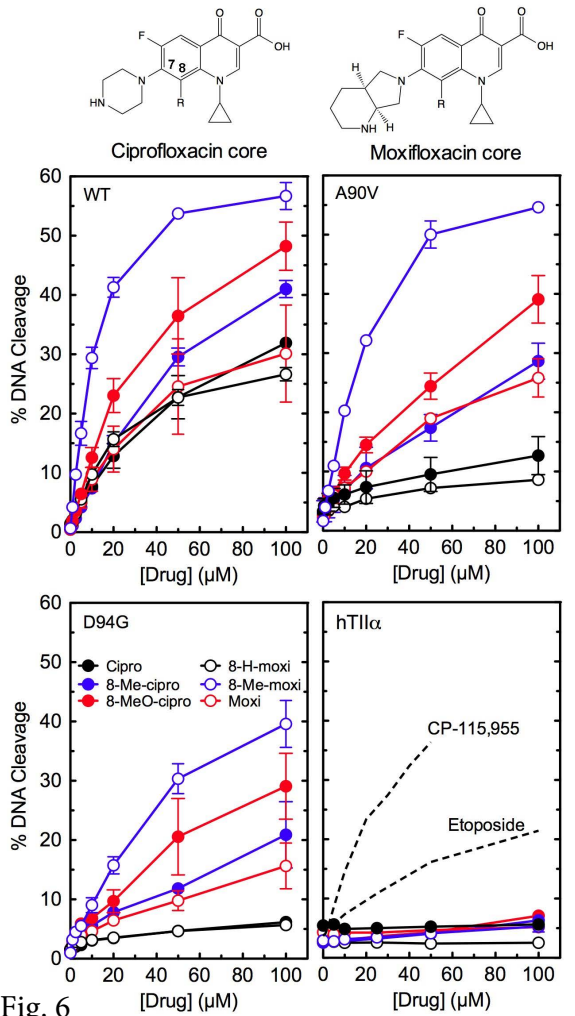
Ciprofloxacin core
Moxifloxacin core
WT
A90V
D94G
hTIIα
% DNA Cleavage
[Drug] (μM)
Cipro
8-Me-cipro
8-MeO-cipro
8-H-moxi
8-Me-moxi
Moxi
CP-115,955
Etoposide

Fig. 6

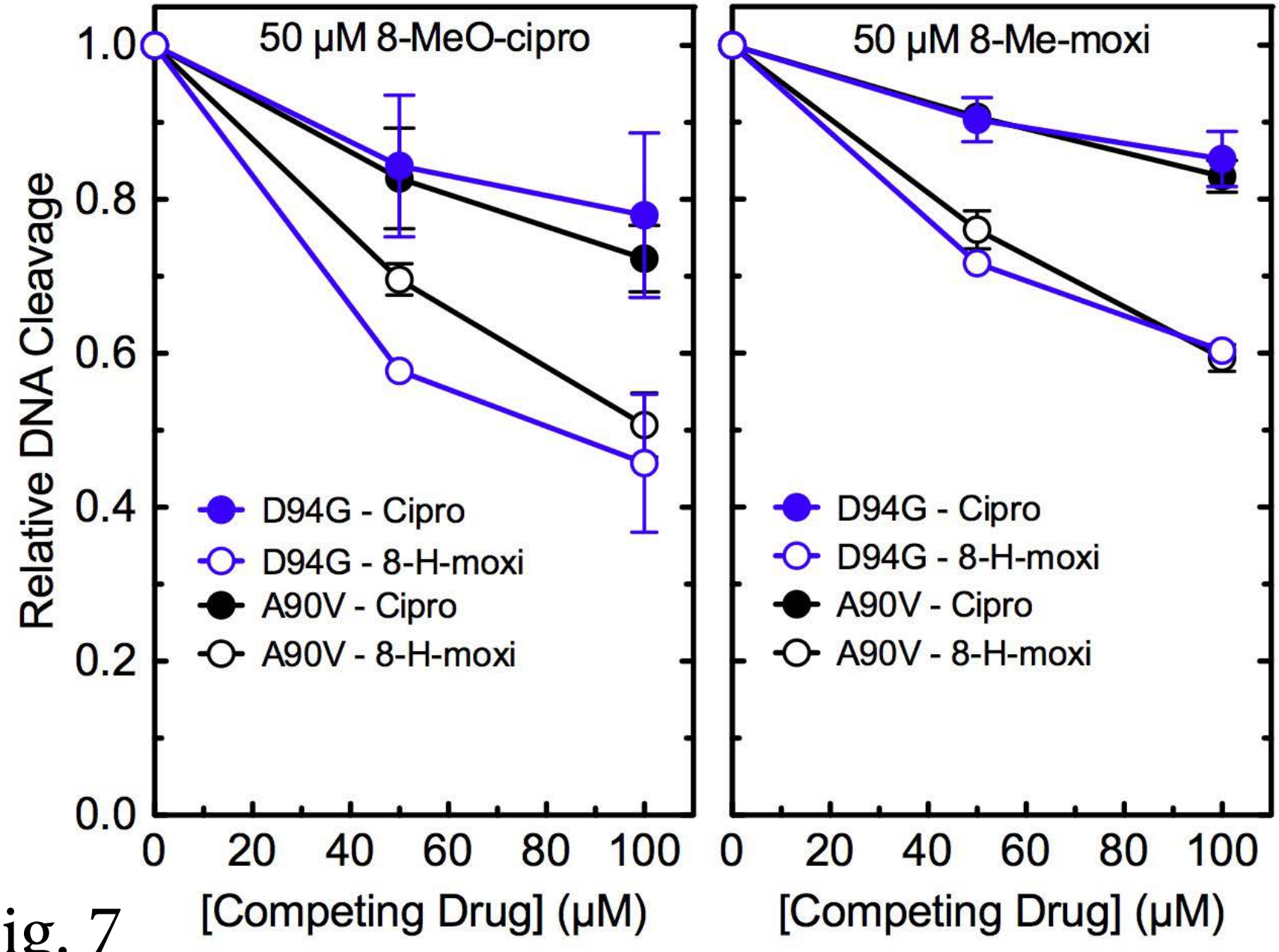
50 μM 8-MeO-cipro
50 μM 8-Me-moxi
Relative DNA Cleavage
1.0
0.8
0.6
0.4
0.2
0.0
0
20
40
60
80
100
[Competing Drug] (μM)
D94G - Cipro
D94G - 8-H-moxi
A90V - Cipro
A90V - 8-H-moxi

Fig. 7

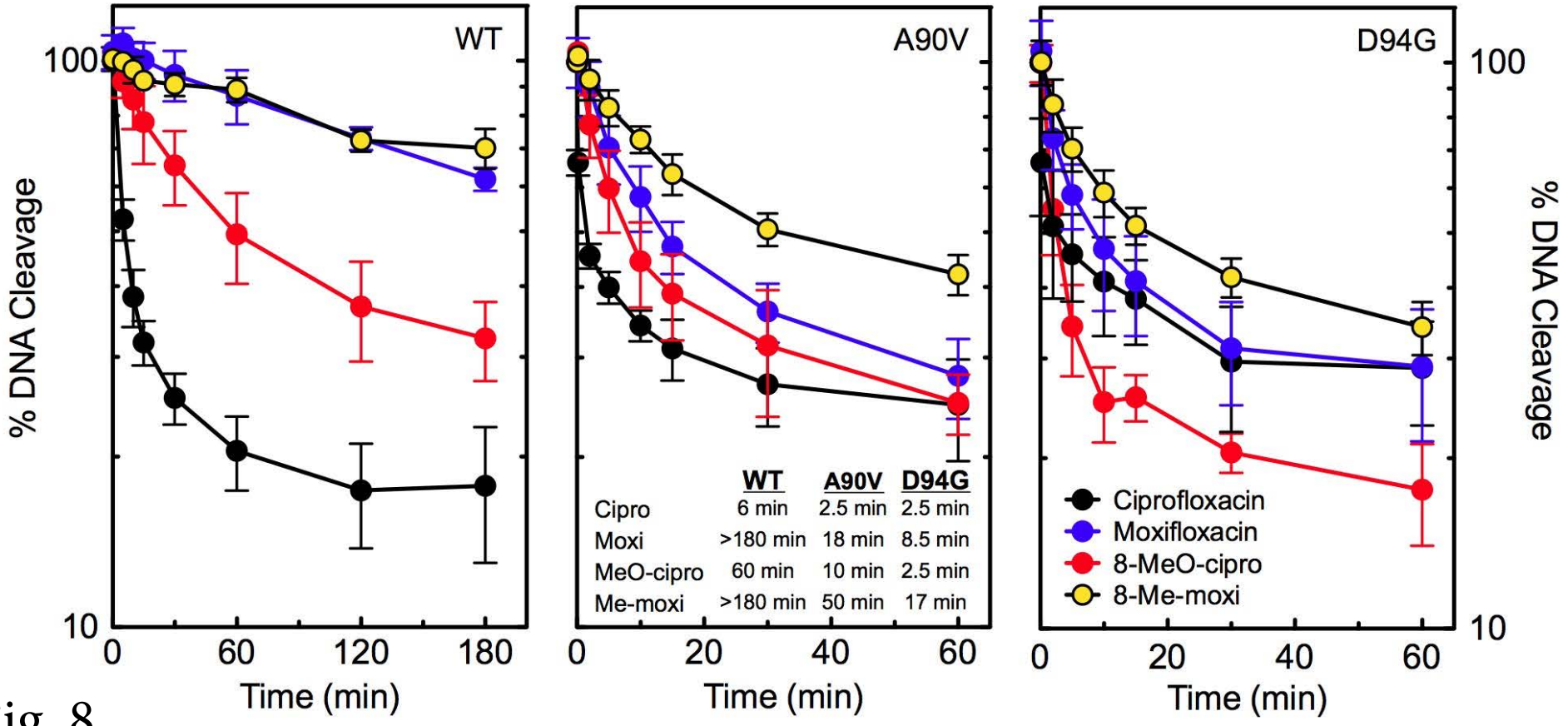
WT
A90V
D94G
100
10
% DNA Cleavage
0
60
120
180
20
40
Time (min)
WT A90V D94G
Cipro 6 min 2.5 min 2.5 min
Moxi >180 min 18 min 8.5 min
MeO-cipro 60 min 10 min 2.5 min
Me-moxi >180 min 50 min 17 min
Ciprofloxacin
Moxifloxacin
8-MeO-cipro
8-Me-moxi

Fig. 8

Supplementary Material

Fluoroquinolone Interactions with *Mycobacterium tuberculosis* Gyrase: Enhancing Drug Activity Against Wild-Type and Resistant Gyrase

Katie J. Aldred, Tim R. Blower, Robert J. Kerns, James M. Berger, and Neil Osheroff

Supplementary Table S1. Full chemical, library, and abbreviated names of compounds used in this study.

Supplementary Figure S2. Effects of moxifloxacin (top) and 8-methyl-moxi (bottom) on DNA cleavage mediated by wild-type (left) and GyrA^{D94G} mutant gyrase (right). The positions of nicked (single-stranded breaks), linear (double-stranded breaks), and the negatively supercoiled (SC) substrate are indicated. Ethidium bromide-stained agarose gels are shown and are representative of three independent experiments.

Supplementary Figure S3. Ability of 50 or 100 µM ciprofloxacin (Cipro) or 50 or 100 µM 8-H-moxifloxacin (8-H-Moxi) to compete out DNA cleavage induced by 50 µM 8-methoxy-cipro with mutant GyrA^{D94G} *M. tuberculosis* gyrase. Cipro or 8-H-moxi and 8-methoxy-cipro were added to reaction mixtures simultaneously. The low level of cleavage seen in the presence of cipro or 8-H-moxi alone is shown at right. Ethidium bromide-stained agarose gels are shown and are representative of three independent experiments.

Name used in this study	Library name	Chemical name
Ciprofloxacin		1-Cyclopropyl-6-fluoro-1,4-dihydro-7-(1-piperazinyl)-4-oxo-3-quinolinecarboxylic acid
8-Methyl-cipro	UILI-2-89	1-Cyclopropyl-6-fluoro-1,4-dihydro-8-methyl-7-(1-piperazinyl)-4-oxo-3-quinolinecarboxylic acid
8-Methoxy-cipro	UIHS-IIa-101	1-Cyclopropyl-6-fluoro-1,4-dihydro-8-methyl-7-(1-piperazinyl)-4-oxo-3-quinolinecarboxylic acid
Moxifloxacin		1-Cyclopropyl-6-fluoro-1,4-dihydro-8-methoxy-7-[(4aS,7aS)-octahydro-6H-pyrrolo[3,4-b]pyridin-6-yl]-4-oxo-3-quinolinecarboxylic acid
8-Methyl-moxi	UIHS-IIa-45	1-Cyclopropyl-6-fluoro-1,4-dihydro-8-methyl-7-[(4aS,7aS)-octahydro-6H-pyrrolo[3,4-b]pyridin-6-yl]-4-oxo-3-quinolinecarboxylic acid
8-H-moxi	UIHS-IIa-239	1-Cyclopropyl-6-fluoro-1,4-dihydro-7-[(4aS,7aS)-octahydro-6H-pyrrolo[3,4-b]pyridin-6-yl]-4-oxo-3-quinolinecarboxylic acid
CP-115,955	CP-115,955	1-Cyclopropyl-6-fluoro-1,4-dihydro-7-(4-hydroxyphenyl)-4-oxo-3-quinolinecarboxylic acid
8-Methyl-3'-(AM)P-FQ	UIHS-I-303	1-Cyclopropyl-6-fluoro-1,4-dihydro-8-methyl-7-[(3S)-3-(aminomethyl)-1-pyrrolidinyl]-4-oxo-3-quinolinecarboxylic acid
8-Methyl-3'-(AM)P-dione	UIJR1-048, Lot UILI-2-95	3-amino-7-[(3S)-3-(aminomethyl)-1-pyrrolidinyl]-1-cyclopropyl-6-fluoro-8-methyl-2,4(1H,3H)-quinazolinedione
8-H-3'-(AM)P-FQ	UIHS-IIIa-35	1-Cyclopropyl-6-fluoro-1,4-dihydro-7-[(3S)-3-(aminomethyl)-1-pyrrolidinyl]-4-oxo-3-quinolinecarboxylic acid
8-H-3'-(AM)P-dione	UIHS-IIa-245	3-amino-7-[(3S)-3-(aminomethyl)-1-pyrrolidinyl]-1-cyclopropyl-6-fluoro-2,4(1H,3H)-quinazolinedione

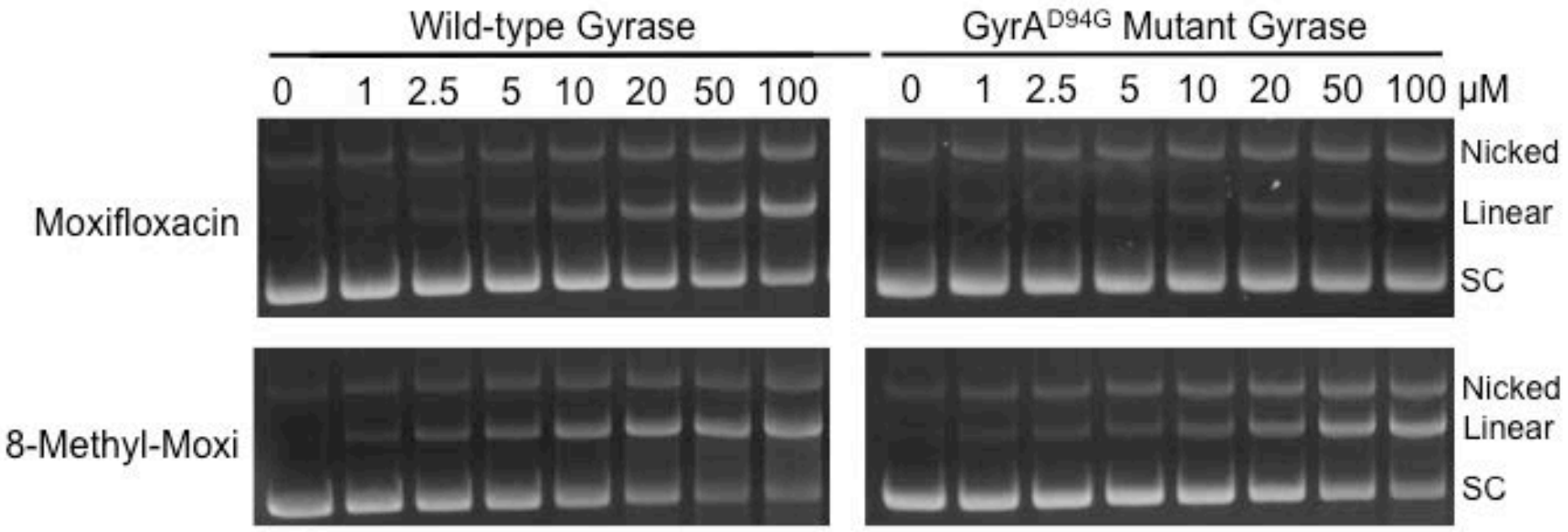
Wild-type Gyrase
GyrA^{D94G} Mutant Gyrase
0 1 2.5 5 10 20 50 100
0 1 2.5 5 10 20 50 100 μM
Moxifloxacin
8-Methyl-Moxi
Nicked
Linear
SC
Nicked
Linear
SC

Fig. S2

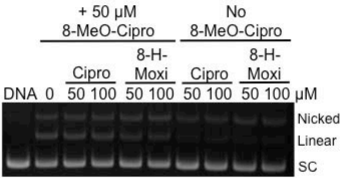
+ 50 μM
8-MeO-Cipro
No
8-MeO-Cipro
Cipro
8-H-
Moxi
Cipro
8-H-
Moxi
DNA 0 50 100 50 100 50 100 50 100 μM
Nicked
Linear
SC

Fig. S3